Polymer 50 (2009) 2357–2364

Contents lists available at ScienceDirect

Polymer

journal homepage: www.elsevier.com/locate/polymer

Synthesis and characterization of fluorescein isothiocyanate (FITC)-labeled PEO–PCL–PEO triblock copolymers for topical delivery

Heui Kyoung Cho [a], Saifullah Lone [a], Dae Duk Kim [b], Joon Ho Choi [b], Sung Wook Choi [c], Jin Hun Cho [d], Jung Hyun Kim [d], In Woo Cheong [a,*]

[a] Department of Applied Chemistry, Kyungpook National University, 1370 Sankyuk-3-dong, Buk-gu, Daegu 702-701, South Korea
[b] College of Pharmacy, Seoul National University, Gwanak-599 Gwanak-ro, Gwanak-gu, Seoul 151-742, South Korea
[c] Department of Biomedical Engineering, Washington University in St. Louis, One Brookings Drive, St. Louis, MO 63130-4899, USA
[d] School of Chemical Engineering and Biotechnology, Yonsei University, 134 Shinchon-dong, Sudaemoon-Ku, Seoul 120-749, South Korea

ARTICLE INFO

Article history:
Received 31 December 2008
Received in revised form
18 March 2009
Accepted 19 March 2009
Available online 27 March 2009

Keywords:
Fluorescein isothiocyanate
Biodegradable
PEO–PCL–PEO

ABSTRACT

We present the synthesis of fluorescein isothiocyanate (FITC)-labeled poly(ethylene oxide)-*block*-poly(ε-caprolactone)-*block*-poly(ethylene oxide) (PEO–PCL–PEO) triblock copolymers and their applications for tracking the penetration behavior of FITC-labeled copolymers in the hairless mouse skin. In the first step, PEO–PCL diblock copolymers with different ratios of PCL to PEO (i.e., [CL]/[EO]) were prepared by ring opening polymerization of ε-caprolactone (CL), where monomethoxy poly(ethylene glycol) (mPEG, $M_n = 2000\ g\ mol^{-1}$) was used as a macro-initiator. FITC was successively reacted with octadecylamine, isophorone diisocyanate (IPDI), and then used as a linker to obtain PEO–PCL–PEO triblock copolymers from the PEO–PCL diblock copolymers. In aqueous solution, both FITC-labeled triblock copolymers show two UV absorption peaks at 489 and 455 nm, attributed to the monomeric FITC and H-aggregated FITC moieties, respectively. Due to the strong H-aggregation of FITC in the copolymer of high [CL]/[EO], fluorescent emission intensities considerably decreased at high concentrations of the copolymer. FITC-labeled copolymers exhibited more sharper polarized optical and fluorescence microscopic images compared to the mixtures of FITC and unlabeled copolymer in both solid crystalline and multiple emulsion state. Furthermore, the Frantz diffusion cell test was carried out to demonstrate the penetration behavior of the FITC-labeled copolymers in the hairless mouse skin.

© 2009 Elsevier Ltd. All rights reserved.

1. Introduction

Copolymers of the biodegradable polymers and poly(ethylene oxide) (PEG or PEO) are versatile, since the topology, molecular weight, and hydrophilic lipophilic balance (HLB) of the copolymers are relatively easy to control. Many researches have reported on the micelles or nanospheres composed of PEGylated (covalent attachment of PEG) biodegradable polymers [1,2]. Most of the studies focused on the encapsulation efficiency, release behavior, long-term circulations in animals, and site-specific drug delivery depending on the characteristics of the copolymers [3–6]. Several reports dealt with the behavior of the copolymers in drug encapsulation or drug delivery; however, the role of the copolymers has not been clearly unearthed until now [7–11].

Labeling fluorescent dyes has been considered as a simple and useful tool for tracking drugs or polymers due to the high sensitivity of fluorescent dyes [6,12]. There have been a number of researches on the dye-labeled drugs or proteins as tracers for targeting and diagnosis of tumor in the biomedical fields [13,14]. Among the fluorescent dyes, fluorescein isothiocyanate isomer (FITC) has been often used. For example, FITC-conjugated deacetylated chitin [5], FITC-labeled human plasma [15], FITC-labeled collagen [16], FITC-conjugated PEO [17] among others, have been reported so far [18–20]. Laibin et al. also studied the internalization of rhodamine-conjugated PEO–PCL diblock copolymers into cells [6]. However, to the best of our knowledge, there have been few studies dealing with FITC-labeled triblock copolymers.

In this study two FITC-labeled PEO–PCL–PEO triblock copolymers with different ratio of PCL to PEO repeating units (i.e., [CL]/[EO]) were synthesized by using a diisocyanate functionalized FITC intermediate. The basic properties of the FITC-labeled triblock copolymers, such as critical micelle concentration (CMC), UV absorption and fluorescent behavior, and crystallization, were investigated and compared with unlabeled triblock copolymers. In addition, we demonstrate the usefulness of the FITC-labeled triblock copolymers as an encapsulation additive as well as a fluorescent probe.

* Corresponding author. Tel.: +82 53 950 7590; fax: +82 53 950 6594.
E-mail address: inwoo@knu.ac.kr (I.W. Cheong).

0032-3861/$ – see front matter © 2009 Elsevier Ltd. All rights reserved.
doi:10.1016/j.polymer.2009.03.032

2. Experimental section

2.1. Materials

ε-Caprolactone (CL, Aldrich Co.) was purified with calcium hydride under vacuum at 70 °C. Monomethoxy poly(ethylene glycol) (mPEG, $M_n = 2000\ g\ mol^{-1}$, Aldrich Co.), fluorescein isothiocyanate isomer I (FITC, Aldrich Co.), octadecylamine (Aldrich Co.), isophorone diisocyanate (IPDI, Aldrich Co.), and hexamethylene diisocyanate (HMDI, Aldrich Co.) were used after removal of moisture under vacuum. Stannous octoate ($SnOct_2$, Aldrich Co.), anhydrous toluene (Aldrich Co.), anhydrous tetrahydrofuran (THF, Aldrich Co.), methylene chloride (MC, Aldrich Co.), Nile Red dye (Aldrich Co.), and diethyl ether (Aldrich Co.) were used without further purification. Pure water (>18.2 MΩ cm, Millipore Co.) was used throughout the experiment. For a skin penetration test, a female hairless mouse (7 weeks old) was used.

2.2. Synthesis

2.2.1. Preparation of PEO–PCL diblock copolymers

The PEO–PCL diblock copolymers were prepared by ring opening polymerization of CL and mPEG in the presence of $SnOct_2$ as described in the literature [4,21]. A schematic regarding the diblock copolymer is illustrated in Fig. 1(a). The formula was designed to fix the M_n of CL units in the diblock copolymers as 1000 and 2500 $g\ mol^{-1}$, respectively (D 2-1 and D 2-2.5, as designated in Table 1). Accordingly, the calculated [CL]/[EO]s

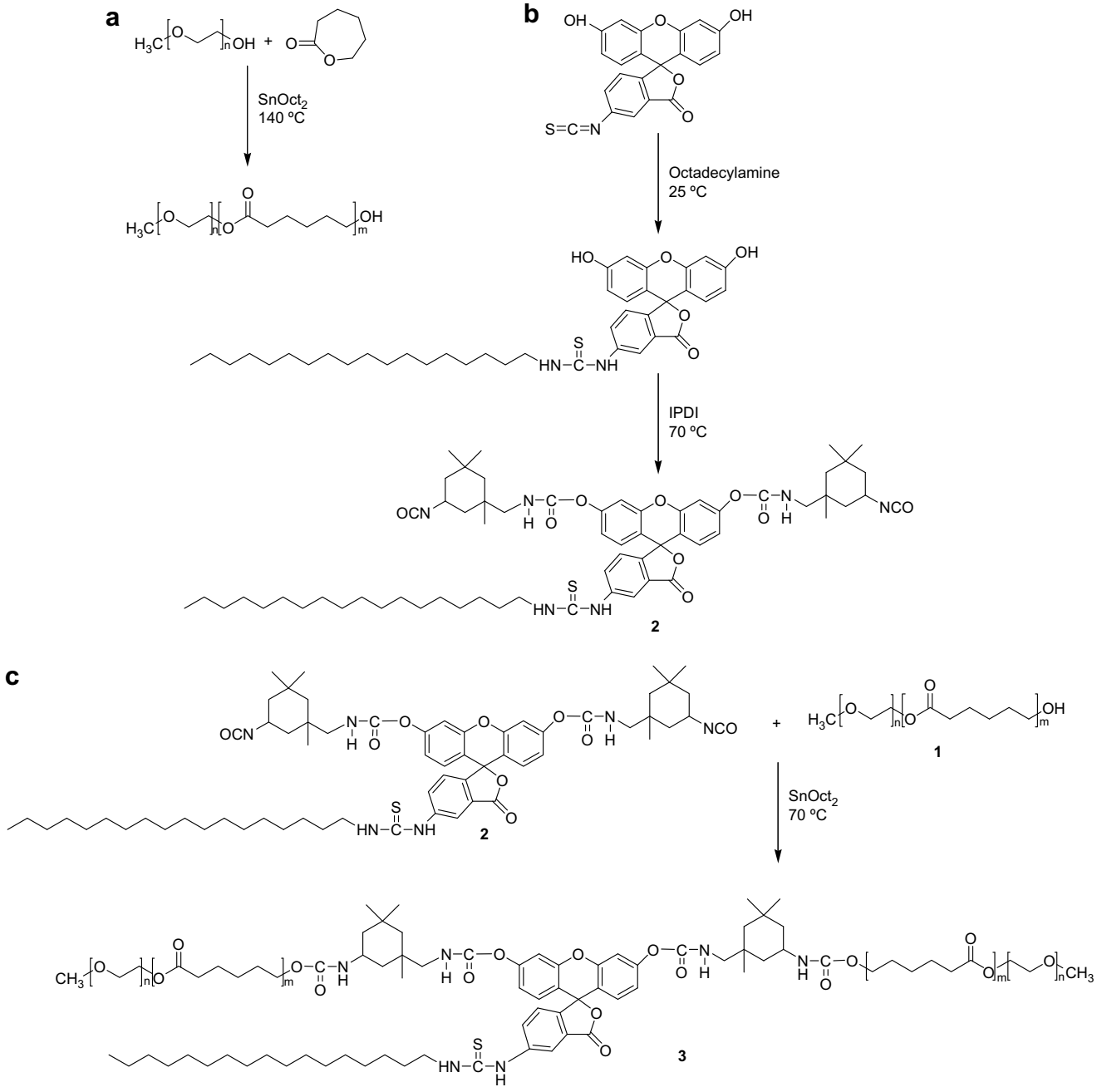

Fig. 1. Schematic of (a) PEO–PCL diblock copolymer (1), (b) chemical modification of FITC with octadecylamine and reaction with IPDI (2), and (c) linkage between (1) and (2) to obtain FITC-labeled PEO–PCL–PEO triblock copolymer (3).

Table 1
The [CL]/[EO] ratio, average molecular weights, PDI ($= M_w/M_n$), and CMC of PEO–PCL diblock and PEO–PCL–PEO triblock copolymers.

Sample ID properties	FITC-labeled triblock copolymers		Unlabeled triblock copolymers		Diblock copolymers	
	FT 2-2-2	FT 2-5-2	T 2-2-2	T 2-5-2	D 2-1	D 2-2.5
[CL]/[EO] exp. (calc.)	0.18 (0.19)	0.53 (0.48)	0.16 (0.19)	0.51 (0.48)	0.15 (0.19)	0.44 (0.48)
M_n[a] (g/mol)	8700	9700	6000	8400	3000	4590
M_n[b] (g/mol)	8120	11,570	6110	6750	4480	6450
M_w[b] (g/mol)	9140	13,520	7180	8700	4970	7000
PDI (–)	1.13	1.17	1.18	1.29	1.11	1.09
CMC[c] (g L^{-1})	0.20	0.12	0.40	0.14	0.15	0.30
HLB[d] (–)	11.2	7.4	13.5	8.3	13.5	8.3

[a] M_n was determined by measuring the relative areas of the peak at 3.65 ppm (EO unit) and the methylene peak at 2.30 ppm (CL unit), respectively, from ^{1}H-NMR (in $CDCl_3$) analysis. For FT 2-2-2 and 2-5-2, the molecular weight (ca. 1100 g/mol) of FITC having octadecylamine moiety was considered.
[b] M_n and M_w were determined by GPC analysis (in THF, with a narrow polystyrene standard of 580–7,500,000 g/mol),
[c] CMC was determined by pyrene UV absorption analysis at 340 nm wavelength.
[d] HLB values were calculated by using Griffin's equation [36]. FITC moiety was considered as the same block as PCL.

based on the formula were 0.19 and 0.48 for D 2-1 and D 2-2.5, respectively. When the [CL]/[EO] was 0.48, for example, 4.03 mmol of mPEG was dissolved completely in 80 mL of anhydrous toluene. Dean stark trap was then conducted to remove residual water for 25 min. Both 88 mmol of CL and 3.98 mmol of $SnOct_2$ were added to the reaction mixture and kept under stirring at 140 °C for 14 h. The product was precipitated in diethyl ether and kept in a refrigerator at 5 °C for 1 day. The supernatant solvent was removed after ultracentrifugation at 14,000 rpm for 3 h, and was followed by vacuum drying.

2.2.2. Preparation of the FITC intermediate

The FITC intermediate was prepared in a stepwise procedure as follows: both 2.01 mmol of FITC and 2.01 mmol of octadecylamine were dissolved in 35 mL of anhydrous THF. The reaction was conducted at room temperature for 1 h under an N_2 atmosphere. 4.03 mmol of IPDI and 3.98 mmol of $SnOct_2$ were then added to the reaction mixture. The reaction was carried out at 60 °C for 3 h under N_2 atmosphere. The chemical modification of FITC is shown in Fig. 1(b).

2.2.3. Preparation of FITC-labeled and unlabeled PEO–PCL–PEO triblock copolymers

The intermediate (2) of the second step was added into that (1) of the first step, and kept under stirring at 60 °C for 8 h under N_2 atmosphere. After the reaction, the final product was obtained through the same purification procedure as described above. The final yield of the triblock copolymers was ca. 80%. Two FITC-labeled copolymers were synthesized as provided in Table 1 (designated as FT 2-2-2 and FT 2-5-2). Preparation of the FITC-labeled copolymer is shown in Fig. 1(c). For the comparative study, two unlabeled copolymers (i.e., T 2-2-2 and T 2-5-2) were synthesized from D 2-1 and D 2-2.5 under the same procedure as shown in the literature [20,22–24]. In the synthesis, HMDI was used as a linker instead of the FITC intermediate. The final yield of the unlabeled triblock copolymers was ca. 83%.

2.3. Characterization

2.3.1. Molecular weights and chemical structure

The number- and weight-average molecular weights (M_n and M_w, respectively) as well as the polydispersity index (PDI, M_w/M_n) of the copolymers were measured by a gel permeation chromatography (GPC) system (OmniSEC, Viscotek Co.) equipped with a refractive index detector (VE-3580), an isocratic pump (VE-1122), and a series of columns (PLgel 5 μm Mixed-C), and conducted at 40 °C. THF was used as an eluent. Calibration was carried out by using narrow polystyrene standards (EasiCal®, Polymer Laboratories Co.) with a range of 580–7,500,000 g mol^{-1}. A 400-MHz NMR spectrometer (^{1}H-NMR in $CDCl_3$, AVANCE digital 400, Bruker Co.) was used to confirm the composition and M_n of the copolymers, where 0.03 vol.% of tetramethylsilane (TMS) was used as an internal standard.

2.3.2. Critical micelle concentration

Critical micelle concentration (CMC) was determined from UV–visible absorption intensity of pyrene ($[Py]_w^{sat} = 10^{-7}$ M at 25 °C) as a function of the copolymer concentration [23].

2.3.3. UV–visible absorption and fluorescence analysis

UV–visible absorption and fluorescent emission of the copolymers were studied by using a UV–visible spectrophotometer (UV-1650PC, Shimadzu Co.) and a fluoro-spectrophotometer (RF-53XPC, Shimadzu Co.), respectively. The copolymer sample was dissolved in pure water and the concentration was recorded from 0.001 to 2.000 g L^{-1}.

2.3.4. Thermal analysis

A differential scanning calorimeter (DSC, Q50, TA Instr. Co.) was used to study the melting (T_m) and crystallization (T_c) temperatures of the copolymers at the rate of 10 °C min^{-1}. The sample size was 10 mg and a heat exchange was recorded during the second cooling cycle.

2.3.5. Spherulite morphology

Polarized optical microscopy (POM, Axioplan 2, Carl Zeiss Co.) and fluorescence microscopy (Axioplan 2, Carl Zeiss Co.) were used to study the spherulite morphology of the copolymers in the dried state. 1 g of the copolymer was dissolved in 1 mL of MC. 2–3 Drops of the solution were dropped onto a slide glass, with cover glass mounted on the glass surface. The sample was heated to 60 °C in a convection oven and cooled to room temperature at the rate of 4 °C h^{-1}. In the case of unlabeled copolymers, FITC (the same moles as the unlabeled copolymer) was dissolved into the aqueous solution of the unlabeled copolymer.

2.3.6. Morphology of multiple emulsions

Confocal laser scanning microscopy (CLSM, MRC 1024/ES, Bio-Rad Co.) was used to study the morphology of water-in-oil-in-water ($W_1/O/W_2$) multiple emulsion droplets in the presence of the copolymers. In preparation of the multiple emulsion, 0.75 g of the FITC-labeled triblock copolymer was added into 2.4 g of pure water and stirred for 1 h at room temperature. The polymer solution (W_1 phase) was poured into 7 g of toluene (O phase, with a trace of Nile Red) and emulsified with a horn-type ultrasonicator (VCX-750, Vibracell Co.) for 2 min under 20 MHz and 21% power. The prepared W_1/O emulsion was poured into 7.8 g of 23 wt.% Tween 60 aqueous solution (W_2 phase), and the mixture was stirred with a homogenizer at 13,500 rpm for 2 min. For the unlabeled copolymers, a trace of FITC was dissolved in the W_1 phase. The final concentration of the copolymer in the $W_1/O/W_2$ multiple emulsion was 3 wt.%. The CLSM images were taken at the excitation wavelengths of 488 and 568 nm, respectively.

2.3.7. Skin penetration

A Frantz diffusion cell (FDC) test was carried out to elucidate the penetration behavior of FITC-labeled triblock copolymers in the mouse skin layer. A receptor chamber (5 mL volume) of the FDC was

filled with PBS buffer solution (pH 7.4) and kept at 32 °C with a thermostat. The skin was peeled off from the hairless mouse, washed with 50 vol.% of ethanol aqueous solution, and located in between the receptor and donor chambers of the FDC. The penetration area of the skin was 0.785 cm^2. The donor chamber was then charged with 1 mL of FT 2-2-2 or FT 2-5-2 aqueous solutions (1 wt.%) and kept for 12 h at 32 °C. After that, the skin was taken from the FDC and embedded in OCT compound (Optimal Cutting Temperature, Tissue-Tak®) to prepare a cryostat microtome sample. Distribution of the FITC-labeled triblock copolymers in the mouse skin was observed by CLSM at 488 nm wavelength.

3. Results and discussion

3.1. Chemical structure and composition

Fig. 2(a) shows a chemical structure of the FITC-labeled PEO–PCL–PEO triblock copolymer, where two PEO–PCL diblock copolymers were linked with the FITC unit having two NCO groups. The unlabeled copolymers (T 2-2-2 or T 2-5-2) were prepared by linking two PEO–PCL diblock copolymers with HMDI. For the effects of PCL chain length, [CL]/[EO] values in the formula were fixed at 0.19 and 0.48 for (F)T 2-2-2 and (F)T 2-5-2, respectively. The average molecular weights, compositions, CMC, and hydrophile–lipophile balance (HLB) of the triblock copolymers are summarized in Table 1.

As shown in Table 1, the values of M_n, M_w, and PDI measured by both GPC and ^{1}H-NMR were coincident with the expected values. The experimental values of [CL]/[EO] obtained from ^{1}H-NMR were comparable to the calculated values based on the formula. The CMC of (F)T 2-5-2 was lower than that of (F)T 2-2-2 due to the high ratio of [CL]/[EO]. There was a little difference in the CMC values between FITC-labeled and unlabeled copolymers, and which probably originated from the FITC moiety. In Fig. 2(b), ^{1}H-NMR spectra of FT 2-2-2 and FT 2-5-2 were shown. The inset represents the chemical shifts of aromatic rings in the FITC moiety. These were detected at 6.66 and 6.72 ppm, respectively, and which were shifted to upfield as compared with those of pure FITC, i.e., 6.32 and 6.38 ppm. The results are attributed to the formation of thiourea bond between octadecylamine and FITC, where the hydrogens in FITC are deshielded by oxygen and nitrogen atoms.

3.2. UV absorption and fluorescence properties

The UV–visible absorption spectra of the FT 2-2-2 and FT 2-5-2 in aqueous solutions were monitored in the range of 400–550 nm. The concentration of FT copolymers was recorded from 0.001 to 2.000 g L^{-1}. The absorption peak of the monomeric FITC molecule (I_{mono}) was observed at 489 nm, and which was very close to the absorption wavelength (492 nm) of pure FITC in an aqueous solution at pH ~7 [25]. The intensity at the maximum absorption wavelength at 489 nm was plotted in Fig. 3(a) as a function of molar concentration (mol L^{-1}). There was no significant difference in the absorption peak intensity between FT 2-2-2 and FT 2-5-2 at low copolymer concentrations. However, the intensity of a secondary absorption peak ($I_{H\text{-}agg}$ at 455 nm) became predominant at increased FT 2-2-2 and FT 2-5-2 concentration. The maximum absorption wavelength shifted from 489 to 455 nm around the CMCs, indicating H-aggregation of FITC [26]. Typically,

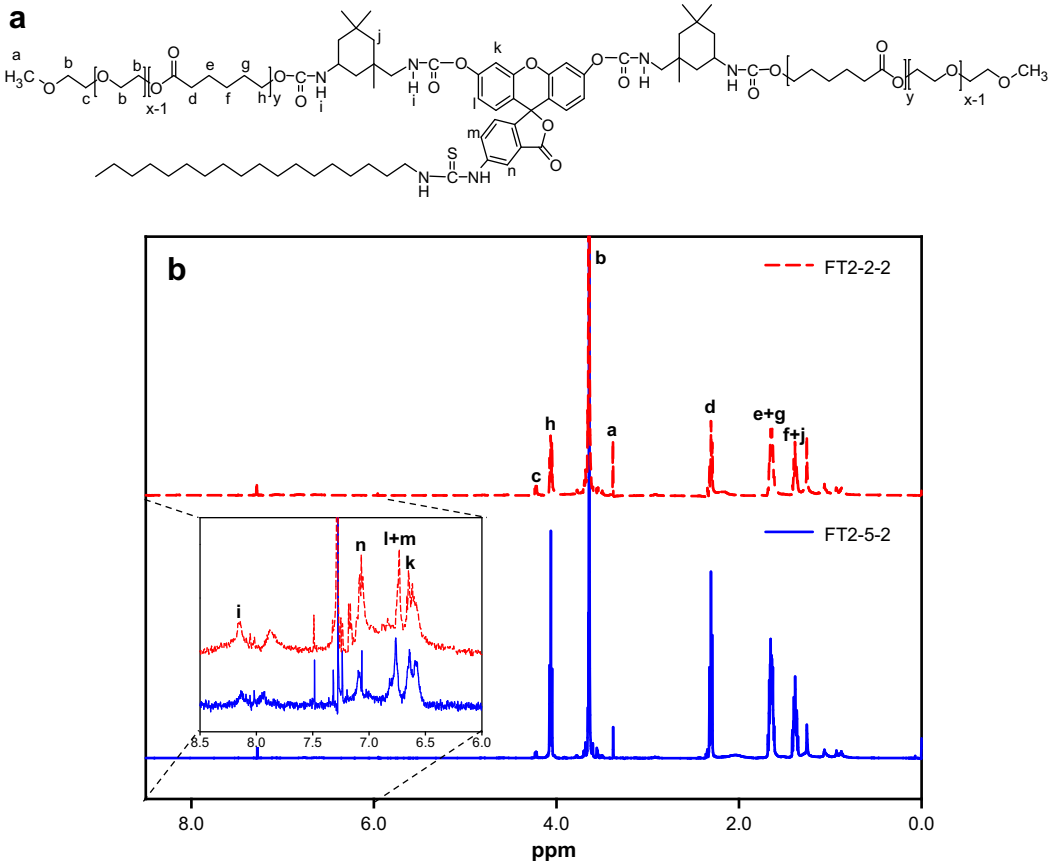

Fig. 2. (a) A chemical structure of the FITC-labeled PEO–PCL–PEO triblock copolymer and (b) ^{1}H NMR spectra of FT 2-2-2 and FT 2-5-2 in $CDCl_3$. The inset represents the chemical shifts of aromatic rings in the FITC moiety.

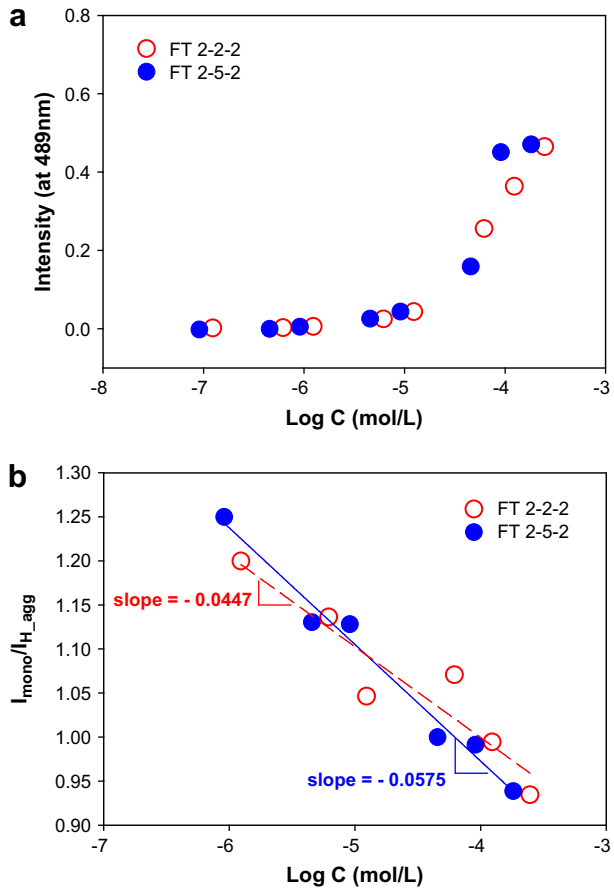

Fig. 3. (a) UV–visible spectra of the FT 2-2-2 and FT 2-5-2 in pure water as a function of the copolymer concentration and (b) the UV absorption intensity ratio of monomeric (I_{mono}, at 489 nm) to H-aggregation ($I_{H\text{-}agg}$, at 455 nm). The dash and solid fitting lines indicate FT 2-2-2 and FT 2-5-2, respectively.

self-association or self-assembly of fluorescent dye molecules can be done by the van der Waals attractive force either in solutions or at interfaces [5,17]. This leads to the substantial change in photophysical properties. As shown in Fig. 3(b), the relative peak intensity change was plotted in terms of the $I_{mono}/I_{H\text{-}agg}$ as a function of the FT copolymer concentrations. It is clearly shown that the slope (-0.0575, $r^2 = 0.98$) of the $I_{mono}/I_{H\text{-}agg}$ in FT 2-5-2 is higher than that (-0.0447, $r^2 = 0.88$) of FT 2-2-2. This implies that FT 2-5-2 tends to form larger aggregates due to the stronger hydrophobic interaction among the longer PCL chains (i.e., high [CL]/[EO]) as compared with FT 2-2-2, and which makes the H-aggregation of FITCs favorable [27]. This can be rationalized in terms of HLB values and aggregate sizes of the copolymers. The calculated HLB values based on Griffin definition were 11.2 and 7.4 for FT 2-2-2 and FT 2-5-2, respectively. At the 1 wt.% concentration, the average aggregate sizes of FT 2-2-2 and FT 2-5-2 were 21 nm ($D_w/D_n = 1.56$) and 24 nm ($D_w/D_n = 1.53$), respectively, and which were measured by a capillary hydrodynamic fractionation (CHDF) at 20 °C.

Fig. 4 exhibits the fluorescent emission intensities (I_{em}) of FT copolymers as a function of the copolymer concentration at 518 nm (excitation $\lambda = 489$ nm). The slopes of two I_{em} gradually increased as the concentration increased up to 0.1 g L^{-1} (1.2×10^{-5} mol L^{-1} and 9.1×10^{-6} mol L^{-1} for FT 2-2-2 and FT 2-5-2, respectively), and which is just below each CMC value. The I_{em}, however, steeply decreased above the CMC values. From the results, the self-quenching of FITC aggregation was confirmed during the

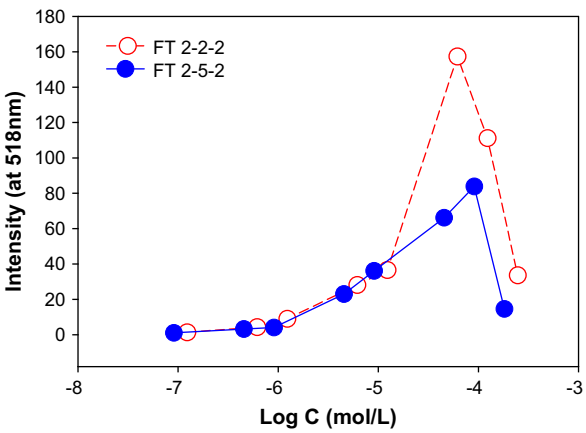

Fig. 4. Fluorescence emission intensity variations of FT 2-2-2 and FT 2-5-2 in pure water as a function of the copolymer concentration. The excitation wavelength was 489 nm.

micellization. Particularly, the I_{em} value of FT 2-5-2 was a half of that of FT 2-2-2 around the CMC. As above-mentioned, aggregate size or aggregation number increases when hydrophobic chain length increases in amphiphilic block copolymers [27,28]. For this reason, FT 2-5-2 showed lower I_{em} values than those of FT 2-2-2 above the CMC. In addition, a long red tail in the raw fluorescence

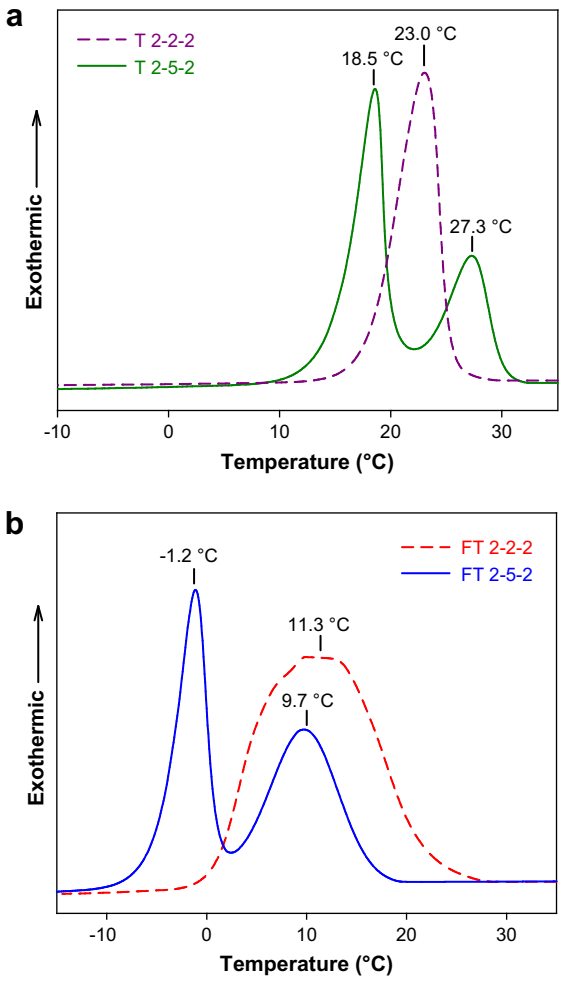

Fig. 5. DSC curves at the 2nd cooling cycle for (a) T 2-2-2 and T 2-5-2, and (b) FT 2-2-2 and FT 2-5-2. The temperatures are the crystalline temperatures (T_c) of PCL or PEO unit.

spectra, which is a typical pattern arising from excimer and H-aggregation, was observed at high concentrations [29].

3.3. Thermal transition

It is well known that thermal behavior of copolymer affects the modulus of drug capsule, release behavior, and its biodegradation rate. Thus, T_m and T_c of the copolymers were investigated using a DSC. In PCL homopolymer ($M_n = 42{,}500$ g mol^{-1}, Aldrich Co.) and mPEG, T_c was observed at 20.5 and 28.0 °C, respectively. It was reported that there was a competitive crystallization between PCL and PEO, depending on their compositions [10,30,31]. For comparison, T_c of both FITC-labeled and unlabeled triblock copolymers was analyzed and their exothermic peaks were shown in Fig. 5. In Fig. 5(a), a narrow T_c regarding PEO in *T* 2-2-2 was detected at 23.0 °C and no T_c in the PCL unit was observed. With respect to *T* 2-5-2, T_c of both PCL and PEO was detected at 27.3 and 18.5 °C, respectively, due to the high [CL]/[EO]. On the other hand, the crystallization transition of PEO in FT 2-2-2 was broadened and the T_c decreased to 11.3 °C from 23.0 °C as shown in Fig. 5(b). In reference to FT 2-5-2, T_c of both PCL and PEO decreased to 9.7 and −1.2 °C, respectively. Such a broad transition of the crystallization and the decrement in T_c in FT copolymers is mainly attributed to the FITC moieties linked between two PCL units. The bulky FITCs interfere with PCL crystallization and lower its T_c value.

3.4. Crystallization behavior

Crystallization behavior of the triblock copolymers was visualized by fluorescence microscopy. As shown in Fig. 6(b), small and luminous PCL crystals are seen among the dark crystal domain of PEO in FT 2-2-2, while the boundaries of PEO lamella are weakly bright. These luminous PCL crystals are attributed to the covalently bonded FITC molecules. For both FT 2-2-2 and T 2-2-2 copolymers, PEO domains are much bigger than those PCL because of the low [CL]/[EO] ratio (0.19) and high crystallization rate of PEO [10,32,33]. The contrast between PEO and PCL domains of FT 2-5-2 seems to be higher than that of T 2-2-2, as shown in Fig. 6(a). In addition, the background is much brighter than the PEO spherulite domain where free FITC aggregates are dispersed.

In the cases of FT 2-5-2 and T 2-5-2, the spherulite sizes of PEO domain become smaller and concentric ring bands consisted of PCL and PEO lamellae are found as shown in Fig. 6(c,d). This is ascribed to the competitive crystal formation between PCL and PEO units at the [CL]/[EO] ratio of 0.48. When both chain lengths of PCL and PEO are comparable, a typical ring-type spherulite can be observed, in which PEO and PCL lamellae are alternatively formed [33,34]. These ring bands are clearly seen only in the POM images (the insets of Fig. 6(c,d)). Such an alternating lamella structure of the ring bands diminishes luminosity of the PCL domains in (F)T 2-5-2 as compared with (F)T 2-2-2.

The spherulite sizes of *T* 2-5-2 are larger than those of FT 2-5-2, as shown in Fig. 6(c,d). This is attributed to the lower T_c value and the existence of bulky FITC moiety in FT 2-5-2. These two factors determine the crystal growth rate of PCL. In the cases of T 2-2-2 and 2-5-2, large aggregates of FITC in yellow color are separated from the spherulite as observed in Fig. 6(a,c). As indicated in Fig. 6(c), the crystal domain of PEO (the arrow in the inset) was too thin to be observed by the POM but it was clearly seen in fluorescence microscopy analysis.

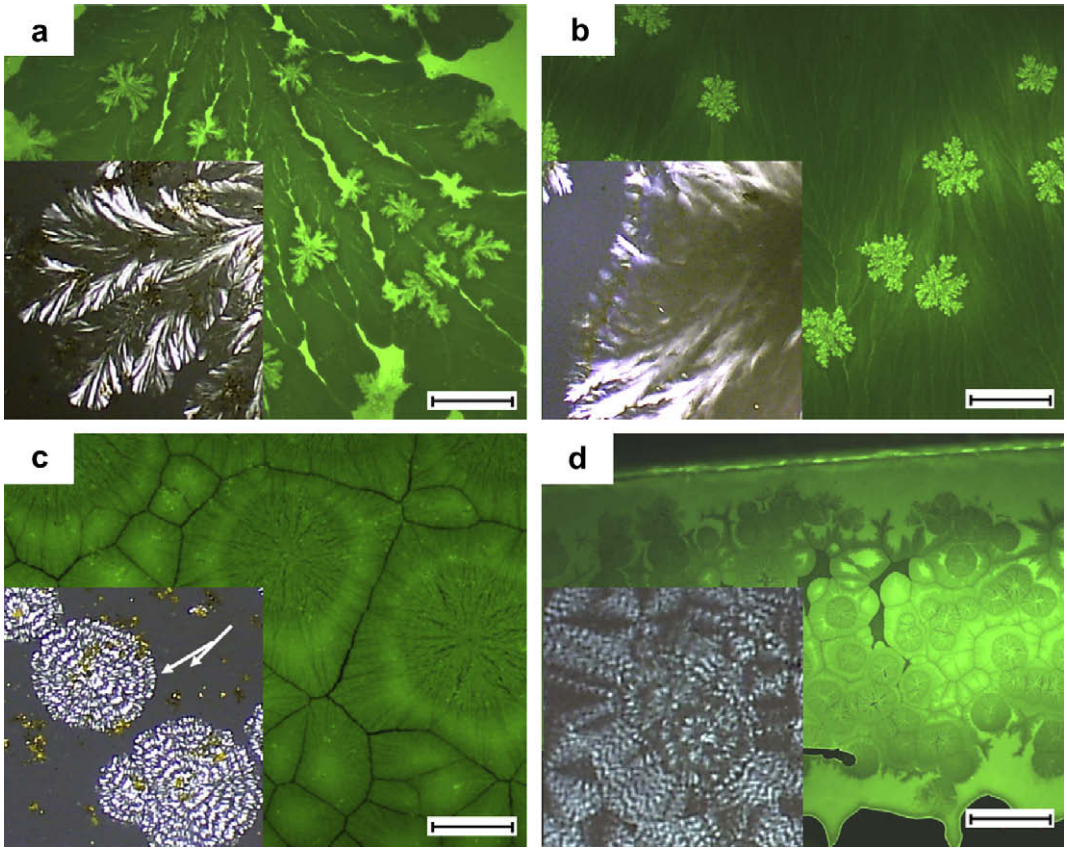

Fig. 6. Fluorescence microscopic images and POM images (insets) of the triblock copolymers: (a) T 2-2-2 with a trace of FITC, (b) FT 2-2-2, (c) T 2-5-2 with a trace of FITC, and (d) FT 2-5-2 (scale bar = 200 μm). The copolymers in MC solution was mounted on the glass substrate and covered with a cover glass. The sample was heated to 60 °C in a forced convective oven, and then cooled down at the rate of 4 °C h^{-1}.

3.5. Morphology of multiple emulsions

A CLSM was used to study the morphology of $W_1/O/W_2$ multiple emulsions in the presence of the triblock copolymers. The copolymers were used as wall materials to stabilize inner water phase. To demonstrate the differences between FITC-labeled and unlabeled copolymers, a trace of FITC was added into the W_1 phase of the emulsion containing unlabeled copolymers. A trace of Nile Red was added into the O phase (toluene). As shown in Fig. 7(b) and (d), the CLSM images of FT copolymers clearly exhibit that W_1 droplets in green color are well dispersed in the oil phase. For the multiple emulsion of T 2-2-2, the entire oil droplet areas containing W_1 droplets are of a yellow color as shown in Fig. 7(a). In particular, free FITCs are observed in the W_2 phase of T 2-5-2, as shown in Fig. 7(c). In the cases of unlabeled copolymers, FITC can easily migrate from W_1 to W_2 phase due to its amphiphilic nature.

3.6. Penetration behavior

Penetration behavior of the FITC-labeled triblock copolymers was investigated with FDC test. Representative CLSM images of mouse skin treated with FITC-labeled copolymers (in green color) were shown in Fig. 8. As shown in Fig. 8(a), most of FT 2-2-2 was located in the stratum corneum layer (thickness = 10–15 μm). On the other hand, some of FT 2-5-2 were penetrated into the epidermis layer (thickness = ~100 μm). In general, penetration rate is closely related to both diffusion rate and solubility in the penetration matrix [35]. The diffusion rate mainly depends on the size of molecule and the solubility can be considered in terms of HLB. Regarding FT 2-2-2 and 2-5-2, the molecular sizes are not so different but their HLB values are significantly different due to the different [CL]/[EO] values.

Topical delivery of substances can be achieved via several pathways such as, hair follicles, sweat ducts, and continuous stratum corneum. The latter can be divided into two potential routes, i.e., transcellular and intercellular routes. The transcellular route is of hydrophilic bundles of keratin and the intercellular route is of amphiphilic crystalline structure of mixed cholesterols, fatty acids, and so on. It is well known that substances having high molecular weights (>500 Da) cannot penetrate via the transcellular route, so amphiphilic block copolymers can penetrate only via the intercellular route depending on their HLB. As shown in Fig. 8(b), FT 2-5-2 of low HLB value can penetrate into the deeper layer of skin than that of FT 2-2-2, although both FT copolymers are located at the stratum corneum layers. This is the evidence that the FT 2-5-2

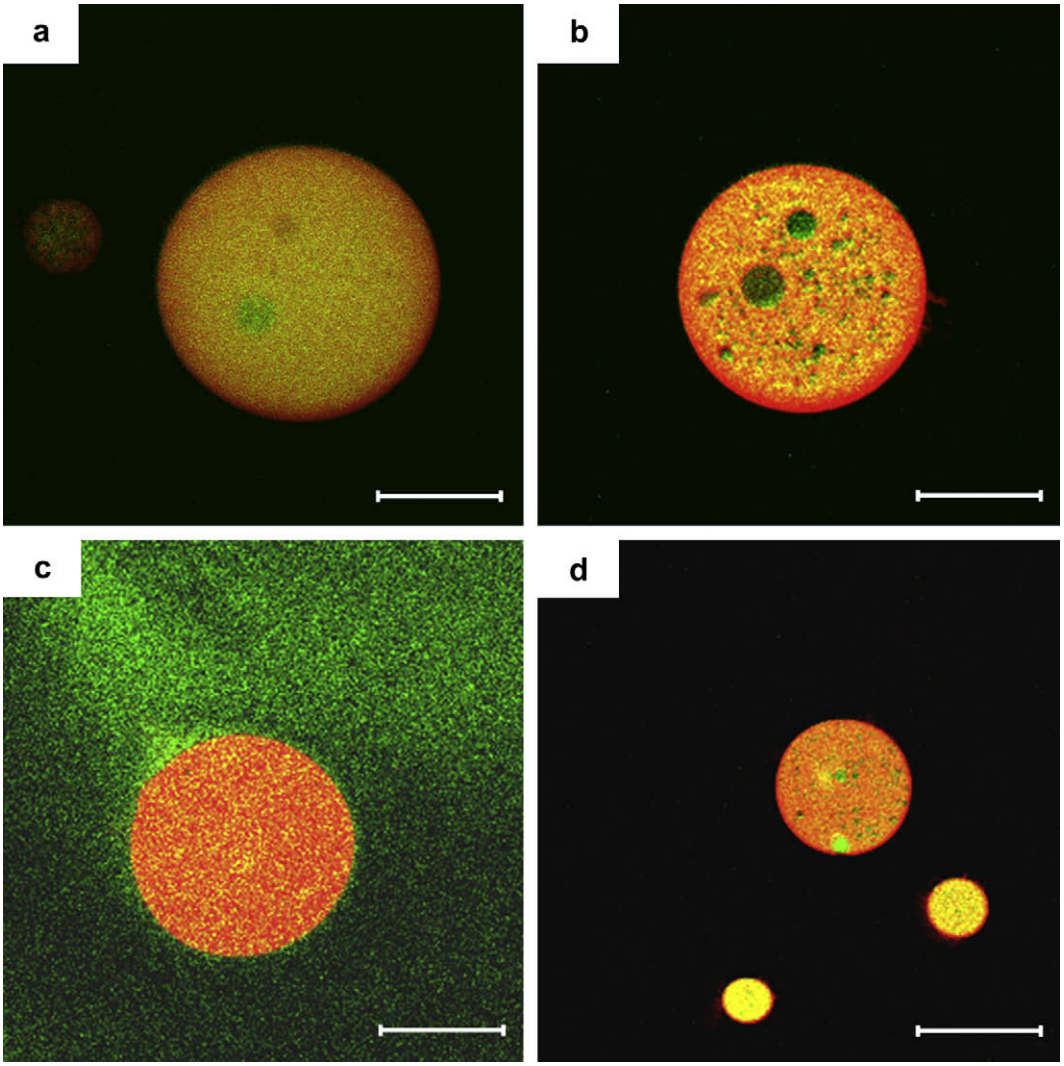

Fig. 7. CLSM images of the multiple emulsions containing FITC-labeled copolymers or unlabeled copolymers with a trace of FITC: (a) T 2-2-2 with a trace of FITC, (b) FT 2-2-2, (c) T 2-5-2 with a trace of FITC, and (d) FT 2-5-2 (scale bar = 100 μm).

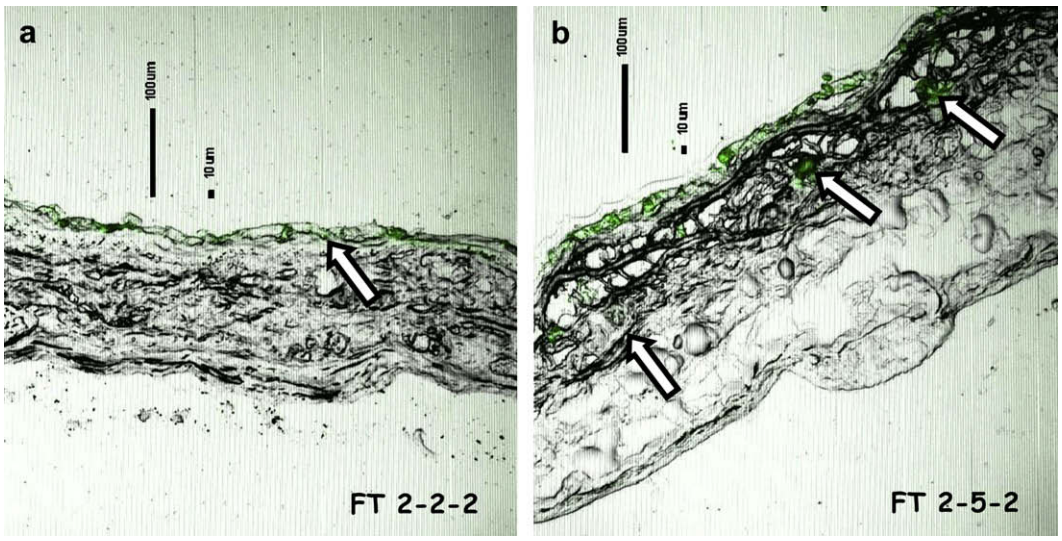

Fig. 8. CLSM images of cross-sectional mouse skin treated with FITC-labeled PEO–PCL–PEO triblock copolymers in a Frantz diffusion cell for 12 h at 32 °C: (a) FT 2-2-2 and (b) FT 2-5-2.

can overcome the barrier of the stratum corneum that prohibits the penetration of external substances. We believe that tracking FITC-labeled copolymers in topical drug delivery would be helpful to elucidate the release behavior of the drugs stabilized by other similar block copolymers.

4. Conclusions

FITC-labeled PEO–PCL–PEO triblock copolymers with different [CL]/[EO] were studied and compared with unlabeled triblock copolymers. FT 2-2-2 and FT 2-5-2 show a typical UV–visible absorption and fluorescence emission behaviors, which are strongly influenced by the copolymer concentration. The addition of FITC leads to a decrease in T_c regarding both PCL and PEO. Particularly, a decrease in the T_c of PCL is attributed to bulky FITC moieties having octadecylamine that effectively interfere with the PCL crystallization process. The FITC moiety affects the spherulite morphology of the copolymers and exhibits clearer CLSM images regarding the $W_1/O/W_2$ multiple emulsions without any migration of FITC. We investigated the penetration depth through hairless mouse skin to demonstrate the penetration behavior of the copolymers depending on their [CL]/[EO] or HLB values. As a conclusion, the FITC-labeled copolymers can be used as fluorescent tracers and are very useful in the investigation of topical drug delivery systems.

Acknowledgement

This work was supported by Ministry of Commerce, Industry and Energy (MOCIE) through the project of NGNT (No. 10024160 and 10024146).

Appendix. Supplementary data

Supplementary data associated with this article can be found in the online version, at doi:10.1016/j.polymer.2009.03.032.

References

[1] Maffei P, Borgia SL, Sforzini A, Yasin A, Ronchi C, Ceschel GC. J Drug Delivery Sci Technol 2004;14:363–72.
[2] Kiyoyama S, Shiomori K, Kawano Y, Hatate YJ. Microencapsulation 2003;20:497–508.
[3] Choi C, Chae SY, Kim T-H, Jang M-K, Cho CS, Nah J-W. Bull Korean Chem Soc 2005;26:523–8.
[4] Ge H, Hu Y, Jiang X, Cheng D, Yuan Y, Bi H, et al. J Pharm Sci 2002;91:1463–73.
[5] Onishi H, Machida Y. Biomaterials 1999;20:175–82.
[6] Luo L, Tam J, Maysinger D, Eisenberg A. Bioconjugate Chem 2002;13:1259–65.
[7] Booth C, Attwood D. Macromol Rapid Commun 2000;21:501–27.
[8] Kim MS, Hyun H, Seo KS, Cho YH, Lee JW, Lee CR, et al. J Polym Sci A 2006;44:5413–23.
[9] Piao L, Dai Z, Deng M, Chen X, Jing X. Polymer 2003;44:2025–31.
[10] Takeshita H, Fukumoto K, Ohnishi T, Ohkubo T, Miya M, Takenaka K, et al. Polymer 2006;47:8210–8.
[11] Li S, Garreau H, Pauvert B, McGrath J, Toniolo A, Vert M. Biomacromolecules 2002;3:525–30.
[12] Geng Y, Discher DE. Polymer 2006;47:2519–25.
[13] Pitschke M, Fels A, Schmidt B, Heiliger L, Kuckert E, Riesner D. Colloid Polym Sci 1995;273:740–52.
[14] Adams KE, Ke S, Kwon S, Liang F, Fan Z, Lu Y, et al. J Biomed Opt 2007:12.024017/1-024017/9.
[15] Hoffmann C, Leroy-Dudal J, Patel S, Gallet O, Pauthe E. Anal Biochem 2008;372:62–71.
[16] Hattori S, Fujisaki H, Kiriyama T, Yokoyama T, Irie S. Anal Biochem 2002;301:27–34.
[17] Liu M, Xie C, Pan H, Pan J, Lu WJ. Chromatogr A 2006;1129:61–6.
[18] Heyder P, Gaipl Udo S, Beyer Thomas D, Voll Reinhard E, Kern Peter M, Stach C, et al. Cytometry A 2003;55:86–93.
[19] Nakayama H, Arakaki A, Maruyama K, Takeyama H, Matsunaga T. Biotechnol Bioeng 2003;84:96–102.
[20] Dias CS, Mitra AK. J Pharm Sci 2000;89:572–8.
[21] Haw J-R, Kim C-H. Kongop Hwahak 1997;8:560–7.
[22] Bae SJ, Suh JM, Sohn YS, Bae YH, Kim SW, Jeong B. Macromolecules 2005;38:5260–5.
[23] Cho G, Glatzhofer DT. J Ind Eng Chem 1997;3:29–36.
[24] Cho HK, Cho KS, Cho JH, Choi SW, Kim JH, Cheong IW. Colloids Surf B 2008;65:61–8.
[25] Cao X, Mello SV, Leblanc RM, Rastogi VK, Cheng T-C, DeFrank JJ. Colloid Surf A 2004;250:349–56.
[26] Kashida H, Asanuma H, Komiyama M. Angew Chem Int Ed 2004;43:6522–5.
[27] Patel S, Lavasanifar A, Choi P. Biomacromolecules 2008;9:3014–23.
[28] Xiong XY, Tam KC, Gan LH. J Appl Polym Sci 2006;100:4163–72.
[29] Veronese FM, Morpurgo M. Farmaco 1999;54:497–516.
[30] Floudas G, Reiter G, Lambert O, Dumas P, Chu B. Polym Mater Sci Eng 1998;79:375–6.
[31] Li L, Meng F, Zhong Z, Byelov D, de Jeu WH, Feijen J. J Chem Phys 2007:126.024904/1-024904/7.
[32] He C, Sun J, Zhao T, Hong Z, Zhuang X, Chen X, et al. Biomacromolecules 2006;7:252–8.
[33] He C, Sun J, Deng C, Zhao T, Deng M, Chen X, et al. Biomacromolecules 2004;5:2042–7.
[34] Shiomi T, Imai K, Takenaka K, Takeshita H, Hayashi H, Tezuka Y. Polymer 2001;42:3233–9.
[35] Akala EO, Okunola O, Pan G. Abstracts, 37th Middle Atlantic Regional Meeting of the American Chemical Society. New Brunswick, NJ, United States; May 22–25 2005. GENE-0772005.
[36] Verdinelli V, Messina PV, Schulz PC, Vuano B. Colloids Surf A 2008;316:131–5.